IF-EWT-based framework for classification of motor imagery EEG signals

Ram Bilas Pachori and Krishnakant Sharma
Department of Electrical Engineering
Indian Institute of Technology Indore
Indore-453552, India
Email: (pachori, phd2301202007)@iiti.ac.in

***Abstract*—In this paper, we present a new framework for motor imagery (MI) classification in brain–computer interface (BCI) systems using electroencephalogram (EEG) signals. The proposed framework employs the iterative filtering–based empirical wavelet transform (IF-EWT) signal decomposition method to decompose EEG signals into modes. Instantaneous amplitude and instantaneous frequency are computed for each mode using Hilbert spectral analysis, and time–frequency (TF) images for each channel are then constructed. To obtain event-related desynchronization and synchronization patterns during MI tasks, the mu (8–14 Hz) and beta (16–30 Hz) bands are extracted from each channel TF image, and then combined to preserve temporal, frequency and spatial domain information for each EEG signal. These combined TF images are used as input to a convolutional neural network (CNN) for classification. The proposed framework is tested on the BCI competition IV Dataset 2b, Experiments are conducted with two-channel and three-channel configurations as input to a CNN, which achieved average classification accuracies of 94.21% and 94.39%, respectively. These results indicate that the proposed method outperforms the other existing methods.**

***Index Terms*—Brain-computer interface (BCI), convolutional neural network (CNN), electroencephalogram (EEG), iterative filtering-based empirical wavelet transform (IF-EWT), motor imagery.**

I. Introduction

Brain-computer interface (BCI) technology allows the brain to communicate directly with a computer or assistive device. It enables the translation of brain signals into actionable commands for external devices [1]. This technology is useful for people with physical disabilities, because it allows them to operate devices using brain signals without requiring physical movement. Non-invasive neuroimaging and brain signal acquisition techniques are useful in the diagnosis and analysis of neurological disorders. Magnetic resonance imaging (MRI) is extensively used for brain imaging and has achieved significant advances through machine learning (ML) and deep learning (DL) algorithms for tumor detection, segmentation, and classification [2], [3], [4]. The BCI systems require real-time monitoring of neural activity, for which electroencephalogram (EEG) is the commonly studied technique due to its high temporal resolution and relatively low cost [1]. EEG signals are generated by the electrical activity of the brain, and the signals recorded during an imagined movement task are referred to as motor imagery (MI) EEG signals [5]. During MI tasks, characteristics changes occurred in the mu and beta bands due to event-related desynchronization (ERD) and event-related synchronization (ERS) [3]. During imagined movement, ERD/ERS is reflected by a decrease in mu rhythm power and an increase in beta rhythm power. These patterns form the neurophysiological basis for MI BCI [1].

However, EEG signals are nonstationary and have very low amplitude and signal-to-noise ratio (SNR), making them difficult to build stable MI-BCI systems [1]. To address these challenges, several advanced signal processing techniques and feature extraction methods have been proposed in the literature [6], [7], [8], [9], [10], [11], [12], [13]. The majority of traditional approaches commonly follow a two-stage framework consisting of feature extraction followed by ML-based classification, such as a reactive frequency band (RFB) approach based on time-frequency (TF) series to extract MI features and classification using a support vector machine (SVM) has been developed in [6]. In [7], wavelet-based features were reduced using principal component analysis, then improved with a Gaussian mixture model, and finally classified using an SVM for MI-EEG recognition. Common spatial pattern (CSP)-based methods combined with particle swarm optimization [8], hybrid attractor metagene with bat optimization [9], and temporally constrained sparse group spatial pattern (TSGSP) [10] have been used to improve classification accuracy (Acc). Additionally, wavelet-CSP methods [13], multi-subband analysis [11], and subject-specific channel selection strategies [12] have been proposed to enhance feature discrimination while reducing computational complexity. These methods usually require manual feature engineering and are less effective when dealing with complex, high-dimensional data. In contrast, DL models learn features automatically, scale better, and handle large datasets more efficiently [14].

In recent years, DL has been frequently utilized for MI classification in EEG-based BCI systems. Several studies have demonstrated the effectiveness of DL techniques such as multi-scale adaptive transfer networks (MSATNet) [15], convolutional neural network (CNN) combined with stacked autoencoders (CNN-SAE) [16], and CNN with sliding window techniques [17] for classifying MI EEG signals in BCI system. In addition, a clustering sparse swarm decomposition method (CSSDM) has been introduced in [18] to improve spectral feature extraction and classify using pretrained DL model. These approaches highlight the potential of advanced signal decomposition and DL techniques in improving MI recognition Acc.

Many DL approaches use time-frequency (TF) images as input to CNN models. These images are typically generated using wavelet transform or short-time Fourier transform (STFT) [14], [16], [19]. However, wavelet-based methods depend on the selection of an appropriate mother wavelet, which can affect performance. Similarly, STFT has constant time and frequency resolutions and fixed window size and type [20]. To overcome these issues, we propose a novel framework for MI EEG signal classification using iterative filtering-based empirical wavelet transform (IF-EWT) [21] and CNN. In this study, an IF-EWT-based TF image representation is proposed, which adaptively captures both time and frequency characteristics of MI-EEG signals. These TF images are then applied to CNN as input for MI-EEG signal classification.

The rest of the paper is organized as follows: Section II describes the EEG dataset and proposed framework for classification of MI tasks. Section III presents the experimental results under different scenarios on publicly available dataset. Section IV concludes the presented work.

II. Dataset and Proposed Framework

This section describes the EEG dataset and details of the proposed framework for MI EEG signal classification. Fig. 1 represents the block diagram of the proposed framework.

A. Dataset and preprocessing

In this study, the BCI Competition IV dataset 2b [22] has been used, which consists of EEG recording from nine subjects performing two MI tasks (left and right hand movement). The EEG signals were recorded from three motor-cortex channels C3, Cz, and C4 at a sampling frequency of 250 Hz and filtered during recording. Each subject participated in five sessions, the first two sessions were recorded without feedback, and the last three sessions were recorded with feedback. In this study, three sessions were used for training and two for testing. Each trial session included a fixation phase, a cue indicating the movement of the imagined hand, four seconds of MI, and a short rest period. EEG signals have a low SNR and are affected by artifacts such as muscle activity and eye movements, which can degrade classification performance. Since the proposed framework constructs TF images using adaptive signal decomposition and employs a CNN for classification, only minimal preprocessing is applied. To enhance the SNR and retain the MI related frequency band, a fourth-order Butterworth band-pass filter in the frequency range of 8–30 Hz has been used [14]. Mean normalization and detrending are performed to remove constant offset and baseline drifts in the EEG signals. In this study, 3 s segments of the EEG signals are extracted from 0.5 s to 3.5 s during the MI task.

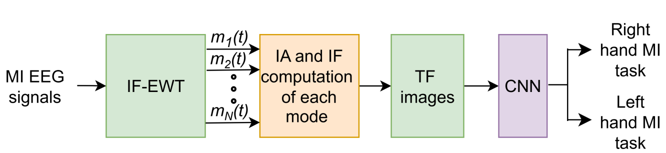

Fig. 1: Block diagram represents the proposed framework of MI EEG signal classification for a BCI system using IF-EWT method with decomposed modes $m_1(t), m_2(t), \ldots, m_N(t)$.

B. IF-EWT-based TF image

In this study, the IF-EWT [21] is employed to decompose the nonstationary EEG signals into a set of meaningful oscillatory modes. The IF-EWT method successively decomposes the signal spectrum using adaptively designed wavelet filters, where the cutoff frequency of Fokker-Planck (FP)-based moving average filter is determined based on the extrema distribution of the signal. The filter length $l = 2 \times \lfloor \alpha \times F_{30}(D_{\text{ext}}) \rfloor$ is automatically computed using the distances between consecutive extrema, enabling effective capture of nonstationary dynamics. where α is scaling parameter, D_{ext} denotes the distances between consecutive extrema and $F_{30}(\cdot)$ is the 30$^{\text{th}}$ percentile. The decomposition process continues until the remaining signal contains three or less than three extrema. A detailed description of the IF-EWT algorithm can be found in [21]. Fig. 2 shows the EEG signal of channel C3 and its corresponding modes obtained by IF-EWT signal decomposition method. Let the EEG signal $x_c(t)$ from channel c be decomposed into N modes $\{m_1(t), m_2(t), \ldots, m_N(t)\}$ using the IF-EWT method. Hilbert spectral analysis (HSA) is then applied to each mode to compute its instantaneous

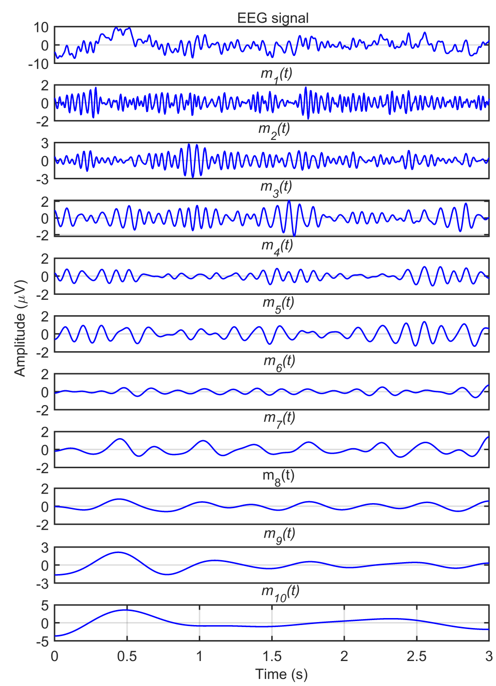

Fig. 2: Time domain representation of channel C3 EEG signal and IF-EWT-based decomposed modes for subject ‘B4’ during the left-hand MI task.

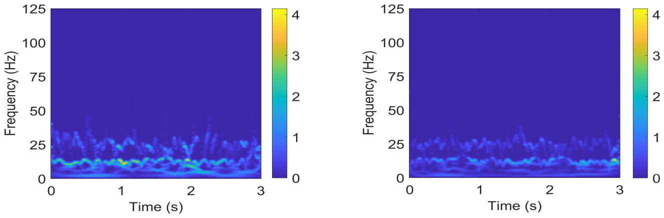

(a) (b)

Fig. 3: TF images of channel C3 for subject 4 during (a) left-hand and (b) right-hand MI tasks.

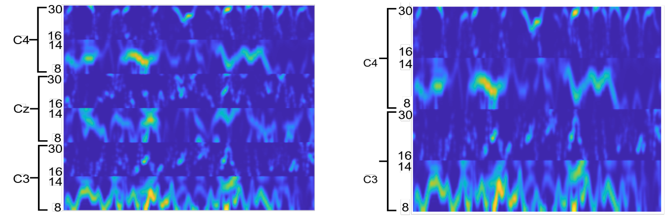

(a) (b)

Fig. 4: Combined TF images of subject B04 during left-hand MI: (a) three-channel combination and (b) two-channel combination.

amplitude (IA) and instantaneous frequency [20]. For the n^{th} mode $m_n(t)$, the analytic signal is defined using the Hilbert transform $\mathcal{H}\{\cdot\}$ as,

$$z_n(t) = m_n(t) + j\,\mathcal{H}\{m_n(t)\} = A_n(t)e^{j\phi_n(t)}. \tag{1}$$

where $A_n(t)$ and $\phi_n(t)$ are IA and instantaneous phase (IP), respectively, and defined as,

$$A_n(t) = \sqrt{m_n^2(t) + [\mathcal{H}\{m_n(t)\}]^2}, \tag{2}$$

$$\phi_n(t) = \tan^{-1}\left(\frac{\mathcal{H}\{m_n(t)\}}{m_n(t)}\right). \tag{3}$$

The instantaneous frequency, denoted by $f_n(t)$, is computed from the time derivative of the IP as,

$$f_n(t) = \frac{1}{2\pi}\frac{d\phi_n(t)}{dt}. \tag{4}$$

The IA and instantaneous frequency obtained from all modes are mapped onto the TF plane. The squared IA values represent the signal energy and each instantaneous frequency is assigned to its nearest frequency bin. This process generates TF images which represent energy variations in the mu and beta bands, enabling the visualization of ERD/ERS patterns during MI tasks [16]. Fig. 3 represents the TF images of the channel C3 for subject B4 during left hand and right hand MI movements. As shown, an ERS pattern is observed in Fig. 3(a), indicated by increased mu band energy in the C3 channel during left-hand MI. Fig. 3(b) shows an ERD pattern, where the mu band energy in the same channel decreases during right-hand MI. The generated TF image has a size of 200 × 200, corresponding to the number of frequency and time samples. The ERD/ERS patterns mainly appear in specific frequency bands. To capture these patterns, the mu and beta frequency bands have been selected. Specifically, the energy in the mu band (8–14 Hz) and the beta band (16–30 Hz) has been extracted from the TF image of each EEG channel [16], [23]. To avoid loss of important information, the frequency ranges of the mu and beta bands were slightly extended. As a result, the extracted mu band image had a size of 39 × 200, while the beta band image had a size of 93 × 200. To keep same effect from both bands, the beta band image was resized to 39 × 200 using cubic interpolation [16]. The mu and beta band images were then combined to form a single image of size 78 × 200. This procedure was applied to all three channels (C3, Cz, and C4).

For CNN input, two configurations were considered, a two-channel configuration using C3 and C4, and a three-channel configuration using C3, Cz, and C4. The stacked TF images had sizes of 156 × 200 for the two-channel configuration and 234 × 200 for the three-channel configuration. Fig. 4 illustrates (a) the three-channel configuration and (b) the two-channel configuration. Finally, the combined TF images for both configurations were resized to 256 × 256 × 3 and given as input to CNN model.

C. Convolutional neural network

CNNs are widely used for image-based classification due to their strong capability to automatically learn discriminative features from input images [24]. In this framework, a lightweight 2D CNN is designed to classify MI EEG signals using the generated TF images as input. The network includes four convolutional blocks followed by two fully connected (FC) blocks. Each convolutional block contains a 2D convolutional layer, batch normalization, and 2×2 max pooling with stride two to reduce the spatial dimensions of the feature maps. The first 2D convolutional layer contains 32 filters with a kernel size of 5×5, while the second, third, and fourth convolutional layers contain 64, 128, and 256 filters, respectively, each with a 3×3 kernel size. A flatten layer is then used to convert the extracted feature maps into a 1D feature vector. The extracted features are passed to the two FC blocks, FC1 and FC2. The first block contains a 128 neurons in FC layer, followed by a dropout layer with a dropout rate of 0.3 to prevent overfitting. The second block contains a FC layer with 2 neurons followed by a softmax layer which produces the MI task classification. The rectified linear unit (ReLU) activation function is used in this study. Fig. 5 represents the detailed architecture of CNN used in this work.

D. Performance measurement

To evaluate the performance of the proposed framework, metrics such as classification Acc, kappa value (Kappa), and F1-score are used [14]. Classification Acc measures the proportion of correctly classified samples and is defined as, Acc $= \frac{TP+TN}{TP+TN+FP+FN}$ where TP, TN, FP, and FN denote true positives, true negatives, false positives, and false negatives, respectively. The kappa value is used to evaluate the classification performance of the algorithm

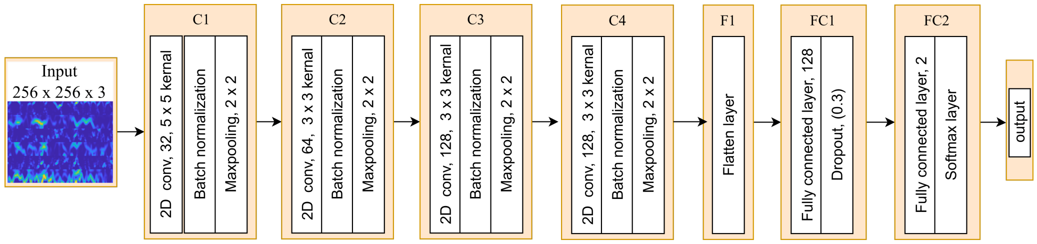

Fig. 5: Architecture of the 2D CNN consisting of convolutional blocks (C1–C4) followed by fully connected layers (FC1 and FC2).

while removing the effect of random classification [16]. It is calculated as, Kappa $= \frac{p_o - p_e}{1-p_e}$ where p_o represents the observed classification Acc and p_e denotes the expected Acc due to random chance. The F1-score is used to measure the balance between precision and recall, and is defined as, F1-score $= \frac{2\times\text{Precision}\times\text{Recall}}{\text{Precision}+\text{Recall}}$ where precision and recall are given by, Precision $= \frac{TP}{TP+FP}$, Recall $= \frac{TP}{TP+FN}$.

III. Results and Discusssion

The performance of the proposed framework is evaluated on BCI Competition IV dataset 2b. The IF-EWT method is applied to decompose the EEG signals into multiple modes. The IA and instantaneous frequency of each mode are then computed using HSA. Based on these features, TF images are generated for each subject and subsequently classified using a CNN model. The input TF images are generated using two-channel (C3–C4) and three-channel (C3–Cz–C4) configurations. The proposed framework is implemented and evaluated on a workstation equipped with an Intel i9 (14th generation) processor, an RTX 4050 GPU with 24 GB memory, and 96 GB of RAM, using MATLAB 2023b. The network is trained using the Adam optimizer with an initial learning rate of 10^{-4}, a mini-batch size of 16, and 120 training epochs. The proposed framework is trained using training session data, where 20% of the training data is kept for validation to monitor the performance of proposed framework and avoid overfitting. The final trained model is then evaluated on unseen test data for each subject.

Table I presents the classification performance of the proposed framework in terms of Acc, kappa value, and F1-score. The highest Acc of 98.57% was achieved for subject 04, indicating the strong discriminative capability of the proposed TF images. In all subjects, the proposed framework achieved average accuracies of 94.21% and 94.39% for the 2-channel and 3-channel combinations, respectively, demonstrating consistent performance. The results indicate that the three-channel configuration slightly improves the classification performance compared to the two-channel configuration.

TABLE I: Classification results of the proposed framework for 2-channel and 3-channel combinations

Subject	2-Channel combination			3-Channel combination		
	Acc (%)	Kappa	F1-score	Acc (%)	Kappa	F1-score
B01	96.50	0.9300	0.9650	94.50	0.8900	0.9450
B02	92.25	0.8450	0.9224	90.50	0.8100	0.9046
B03	90.25	0.8050	0.9025	90.75	0.8150	0.9075
B04	98.33	0.9667	0.9833	98.57	0.9714	0.9857
B05	94.76	0.8952	0.9476	95.24	0.9048	0.9524
B06	95.50	0.9100	0.9550	94.25	0.8850	0.9425
B07	91.25	0.8250	0.9125	94.75	0.8950	0.9475
B08	94.09	0.8818	0.9409	95.91	0.9182	0.9591
B09	95.00	0.9000	0.9500	95.00	0.9000	0.9500
Average	94.21	0.8843	0.9421	94.39	0.8877	0.9438

Table II compares the performance of the proposed framework with existing state-of-the-art methods evaluated on the same dataset. The experiment results show that the proposed method has outperformed to existing methods such as CNN-SAE, frequency-spatial-temporal multidomain, simplified CNN, TSGSP, common average reference with STFT, and MSATNet, on average Acc. The highest accuracy of 98.57% was achieved for subject 04, indicating that the proposed TF images can effectively distinguish different classes. All subjects achieved Acc above 90% which is showing consistent performance across subjects $B01, B02, \ldots, B09$.

Based on the experiment results, the IF-EWT-based TF image framework effectively captures mu and beta band energy variations in MI EEG signals. The TF image obtained by proposed framework provides informative features for CNN-based classification. The comparison between the 2-channel and 3-channel configuration shows that adding channel Cz can enhance the discriminative power for some subjects, but good performance can still be achieved with only 2-channel. Overall, the proposed IF-EWT-based TF image framework is the best framework among all the considerable framework which can effectively classify left hand and right hand MI tasks.

IV. Conclusion

In this work, a novel TF image generation method based on IF-EWT is proposed for MI EEG signal classification. The IF-EWT method is applied to decompose each EEG signal into modes. The IA and instantaneous frequency of each modes are extracted using the HSA. Based on these IA and instantaneous frequency, TF images are constructed which essentially provide time and frequency domain characteristics of the MI EEG signals. The TF images obtained from the C3–C4 and C3–Cz–C4 channel combinations are stacked and used as input to a CNN for feature learning and binary MI classification. The experimental results have shown that the proposed IF-EWT-based TF image improves the MI EEG signal classification

TABLE II: Comparison of the proposed IF-EWT based method with state-of-the-art methods on BCI Competition IV-2b dataset

Method	S1 (%)	S2 (%)	S3 (%)	S4 (%)	S5 (%)	S6 (%)	S7 (%)	S8 (%)	S9 (%)	Average (%)
Tabar et al. [16] (2017)	76.00	65.80	75.30	95.30	83.00	79.50	74.50	75.30	73.30	77.56
Ma et al. [25] (2019)	83.00	61.10	64.60	100.00	95.00	82.90	91.20	90.90	97.00	85.08
Feng et al. [19] (2020)	74.70	81.30	68.10	96.30	92.50	86.90	73.40	91.60	84.40	83.69
Zang et al. [10] (2019)	84.00	62.90	56.30	99.40	94.80	83.80	94.10	93.30	90.10	84.30
Hu et al. [15] (2023)	81.87	72.14	87.81	97.81	99.38	88.44	93.13	94.37	89.60	89.39
Atla et al. [14] (2024)	93.52	89.54	88.75	92.95	93.86	91.81	93.52	91.70	90.11	91.75
Singh et al. [17] (2025)	71.04	66.76	82.31	96.33	86.45	81.19	90.06	87.61	83.92	82.19
Bouchne et al. [26] (2025)	89.81	78.33	74.69	98.56	96.62	90.50	86.90	94.53	93.19	89.24
Proposed (2-Channel)	96.50	92.25	90.25	98.33	94.76	95.50	91.25	94.09	95.00	94.21
Proposed (3-Channel)	94.50	90.50	90.75	98.57	95.24	94.25	94.75	95.91	95.00	94.39

performance, with the three-channel configuration outperforming the two-channel configuration. Overall, the IF-EWT-based TF representation provides an effective approach for capturing the non-stationary dynamics of MI EEG signals, which enhances classification performance. In future, the proposed framework can be studied on a wide EEG database with large number of subjects and computational complexity of the proposed method can be compared with other existing methods in the literature. The hardware implementation of the proposed framework can be studied as a part of the future work. The proposed methodology can be studied for analysis and classification of other biomedical signals associated with the normal and abnormal categories. It would be of interest to develop new EEG signal analysis techniques, features, and classification methods in the proposed framework. The computational complexity of the suggested framework can be reduced as a part of the future work in order to use it in real-life applications.

References

[1] K. Das and R. B. Pachori, "Electroencephalogram-based motor imagery brain–computer interface using multivariate iterative filtering and spatial filtering," *IEEE Transactions on Cognitive and Developmental Systems*, vol. 15, no. 3, pp. 1408–1418, 2022.

[2] M. Balwant, "A review on convolutional neural networks for brain tumor segmentation: methods, datasets, libraries, and future directions," *IRBM*, vol. 43, no. 6, pp. 521–537, 2022.

[3] P. Dequidt, P. Bourdon, B. Tremblais, C. Guillevin, B. Gianelli, C. Boutet, J.-P. Cottier, J.-N. Vallée, C. Fernandez-Maloigne, and R. Guillevin, "Exploring radiologic criteria for glioma grade classification on the BraTS dataset," *IRBM*, vol. 42, no. 6, pp. 407–414, 2021.

[4] M. O. Khairandish, M. Sharma, V. Jain, J. M. Chatterjee, and N. Jhanjhi, "A hybrid CNN-SVM threshold segmentation approach for tumor detection and classification of MRI brain images," *IRBM*, vol. 43, no. 4, pp. 290–299, 2022.

[5] K. Samanta, S. Chatterjee, and R. Bose, "Cross-subject motor imagery tasks EEG signal classification employing multiplex weighted visibility graph and deep feature extraction," *IEEE Sensors Letters*, vol. 4, no. 1, pp. 1–4, 2019.

[6] S. Bhattacharyya and M. K. Mukul, "Reactive frequency band based movement imagery classification," *Journal of Ambient Intelligence and Humanized Computing*, pp. 1–14, 2018.

[7] D. Lee, S.-H. Park, and S.-G. Lee, "Improving the accuracy and training speed of motor imagery brain–computer interfaces using wavelet-based combined feature vectors and Gaussian mixture model-supervectors," *Sensors*, vol. 17, no. 10, p. 2282, 2017.

[8] D. Li, H. Zhang, M. S. Khan, and F. Mi, "A self-adaptive frequency selection common spatial pattern and least squares twin support vector machine for motor imagery electroencephalography recognition," *Biomedical Signal Processing and Control*, vol. 41, pp. 222–232, 2018.

[9] S. Selim, M. M. Tantawi, H. A. Shedeed, and A. Badr, "A CSP\AM-BA-SVM approach for motor imagery BCI system," *IEEE Access*, vol. 6, pp. 49 192–49 208, 2018.

[10] Y. Zhang, C. S. Nam, G. Zhou, J. Jin, X. Wang, and A. Cichocki, "Temporally constrained sparse group spatial patterns for motor imagery BCI," *IEEE Transactions on Cybernetics*, vol. 49, no. 9, pp. 3322–3332, 2018.

[11] S. Kumar, A. Sharma, and T. Tsunoda, "An improved discriminative filter bank selection approach for motor imagery EEG signal classification using mutual information," *BMC Bioinformatics*, vol. 18, no. Suppl 16, p. 545, 2017.

[12] P. Gaur, K. McCreadie, R. B. Pachori, H. Wang, and G. Prasad, "An automatic subject specific channel selection method for enhancing motor imagery classification in EEG-BCI using correlation," *Biomedical Signal Processing and Control*, vol. 68, p. 102574, 2021.

[13] E. A. Mousavi, J. J. Maller, P. B. Fitzgerald, and B. J. Lithgow, "Wavelet common spatial pattern in asynchronous offline brain computer interfaces," *Biomedical Signal Processing and Control*, vol. 6, no. 2, pp. 121–128, 2011.

[14] K. G. R. Atla and R. Sharma, "Motor imagery classification using a novel CNN in EEG-BCI with common average reference and sliding window techniques," *Alexandria Engineering Journal*, vol. 120, pp. 532–546, 2025.

[15] L. Hu, W. Hong, and L. Liu, "MSATNet: multi-scale adaptive transformer network for motor imagery classification," *Frontiers in Neuroscience*, vol. 17, p. 1173778, 2023.

[16] Y. R. Tabar and U. Halici, "A novel deep learning approach for classification of EEG motor imagery signals," *Journal of Neural Engineering*, vol. 14, no. 1, p. 016003, 2016.

[17] K. Singh, N. Singha, G. Jaswal, and S. Bhalaik, "A novel CNN with sliding window technique for enhanced classification of MI-EEG sensor data," *IEEE Sensors Journal*, vol. 25, no. 3, pp. 4777–4786, 2024.

[18] S. V. Bhalerao and R. B. Pachori, "Clustering sparse swarm decomposition for automated recognition of upper limb movements from nonhomogeneous cross-channel EEG signals," *IEEE Sensors Letters*, vol. 8, no. 1, pp. 1–4, 2023.

[19] F. Li, F. He, F. Wang, D. Zhang, Y. Xia, and X. Li, "A novel simplified convolutional neural network classification algorithm of motor imagery EEG signals based on deep learning," *Applied Sciences*, vol. 10, no. 5, p. 1605, 2020.

[20] R. B. Pachori, *Time-frequency analysis techniques and their applications*. CRC Press, 2023.

[21] A. Nalwaya, V. K. Singh, and R. B. Pachori, "Emotion identification from physiological signals using iterative filtering-based empirical wavelet transform," *IEEE Sensors Journal*, pp. 1–1, 2025.

[22] R. Leeb, C. Brunner, G. Müller-Putz, A. Schlögl, and G. Pfurtscheller, "BCI competition 2008–graz data set b," *Graz University of Technology, Austria*, vol. 16, pp. 1–6, 2008.

[23] V. Bajaj and R. B. Pachori, "Automatic classification of sleep stages based on the time-frequency image of EEG signals," *Computer Methods and Programs in Biomedicine*, vol. 112, no. 3, pp. 320–328, 2013.

[24] R. He, K. Wang, N. Zhao, Y. Liu, Y. Yuan, Q. Li, and H. Zhang, "Automatic detection of atrial fibrillation based on continuous wavelet transform and 2D convolutional neural networks," *Frontiers in Physiology*, vol. 9, p. 1206, 2018.

[25] Y. Ma, X. Wu, L. Zheng, P. Lian, Y. Xiao, and Z. Yi, "Iterative outlier removal clustering based time-frequency-spatial feature selection for binary EEG motor imagery decoding," *IEEE Transactions on Instrumentation and Measurement*, vol. 71, pp. 1–14, 2022.

[26] M. Bouchane, W. Guo, and S. Yang, "High-resolution time-frequency feature selection and EEG augmented deep learning for motor imagery recognition," *Electronics*, vol. 14, no. 14, p. 2827, 2025.